Pitchfork bifurcation and circuit implementation of a novel Chen hyper-chaotic system*

Dong En-Zeng(董恩增)[a)b)†], Chen Zeng-Qiang(陈增强)[a)],
Chen Zai-Ping(陈在平)[b)], and Ni Jian-Yun(倪建云)[b)]

[a)] *Department of Automation, Nankai University, Tianjin* 300071, *China*
[b)] *Department of Automation, Tianjin University of Technology, Tianjin* 300384, *China*

(Received 6 October 2011; revised manuscript received 19 October 2011)

In this paper, a novel four dimensional hyper-chaotic system is coined based on the Chen system, which contains two quadratic terms and five system parameters. The proposed system can generate a hyper-chaotic attractor in wide parameters regions. By using the center manifold theorem and the local bifurcation theory, a pitchfork bifurcation is demonstrated to arise at the zero equilibrium point. Numerical analysis demonstrates that the hyper-chaotic system can generate complex dynamical behaviors, e.g., a direct transition from quasi-periodic behavior to hyper-chaotic behavior. Finally, an electronic circuit is designed to implement the hyper-chaotic system, the experimental results are consist with the numerical simulations, which verifies the existence of the hyper-chaotic attractor. Due to the complex dynamic behaviors, this new hyper-chaotic system is useful in the secure communication.

Keywords: hyper-chaos, Chen system, pitchfork bifurcation, center manifold theorem

PACS: 05.45.–a, 05.45.Jn, 05.45.Pq **DOI:** 10.1088/1674-1056/21/3/030501

1. Introduction

In recent years, research into chaos has made remarkable progress in nonlinear science,[1−3] engineering, and other fields.[4−8] Chaos can be beneficial to many real-world applications, such as secure communication,[9−10] fluid mixing, and some other engineering applications.[11−12] Hyper-chaos characterized with more than one positive Lyapunov exponents expands in two or more directions simultaneously, which indicates that hyper-chaos has more complex dynamical behaviors than chaos. This property gives hyper-chaos a broader application prospect in secure communication and other chaos-based fields. Recent research on hyper-chaos is mainly concerned with the generation of hyper-chaotic systems,[13−16] e.g., Yu *et al.* investigated multi-scroll hyper-chaotic attractors in four dimensional systems;[17] Liu *et al.* designed a circuit of a novel autonomous hyper-chaotic system;[18] Qi *et al.* presented a new hyper-chaotic system, which has two large positive Lyapunov exponents.[19]

The bifurcation analysis of hyper-chaotic systems is challenging work, because of their higher dimensions and complexities. However, it is meaningful to analyze the bifurcation phenomena of hyper-chaotic systems. In this paper, the pitchfork bifurcation of a new four-dimensional hyper-chaotic system is investigated.

By using the center manifold theorem and the bifurcation theory, a pitchfork bifurcation is demonstrated to arise at the zero equilibrium point. Besides, by means of numerical simulations, rich dynamical behaviors are found in this system. Moreover, for engineering applications, a circuit implementing this hyper-chaotic system is designed. The experimental results show great consistence with the numerical simulations.

2. Novel Chen hyper-chaotic system

In 1999, the famous Chen system was discovered.[20] By introducing a new state variable w and coupling it to the second equation of the Chen system,

*Project supported by the Natural Science Foundation of China (Grant Nos. 61174094, 50977063, and 60904063), the Foundation of the Application Base and Frontier Technology Research Project of Tianjin, China (Grant No. 10JCZDJC23100), the Development of Science and Technology Foundation of the Higher Education Institutions of Tianjin, China (Grant No. 20080826).

†Corresponding author. E-mail: dongenzeng@163.com

© 2012 Chinese Physical Society and IOP Publishing Ltd

a novel four-dimensional Chen hyper-chaotic system was coined, its mathematical model reads

$$\begin{aligned}\dot{x} &= a(y-x),\\ \dot{y} &= cx + hy - xz - w,\\ \dot{z} &= xy - dz,\\ \dot{w} &= xz + ew,\end{aligned} \tag{1}$$

where $(x, y, z, w) \in \mathrm{R}^4$, and a, c, d, e, h are all real constant parameters and assumed to be positive. This new system contains two quadratic terms and five system parameters. With appropriate parameters, system (1) may have two positive Lyapunov exponents, one zero Lyapunov exponent, and one negative Lyapunov exponent, which means that system (1) is hyper-chaotic. For example, when $a = 35$, $c = 7$, $d = 6$, $e = 2$, $h = 12$, system (1) has two positive Lyapunov exponents, the hyper-chaotic attractors are shown in Fig. 1.

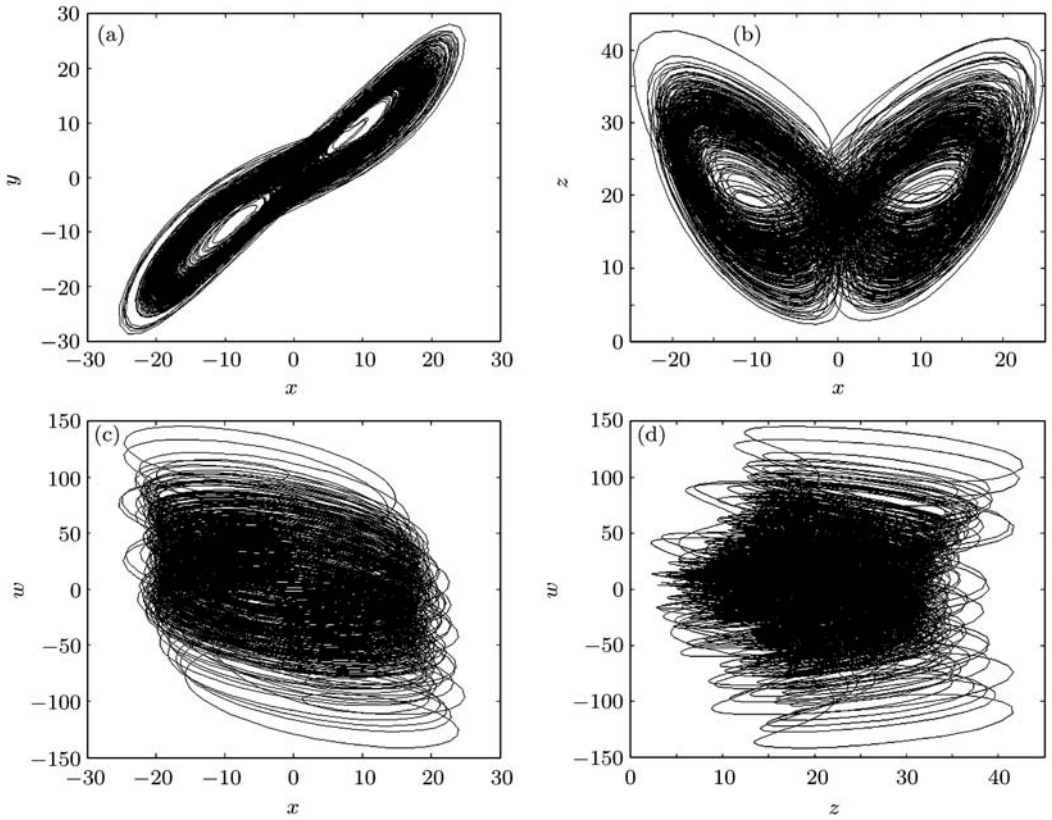


Fig. 1. Hyper-chaotic attractors for system (1) with $a = 35$, $c = 7$, $d = 6$, $e = 2$, $h = 12$ in (a) x–y, (b) x–z, (c) x–w, (d) z–w planes.

2.1. Equilibrium

By solving the following equations:

$$a\,(y-x) = 0, \quad cx + hy - xz - w = 0, \quad xy - dz = 0, \quad ew + xz = 0, \tag{2}$$

we can easily find that system (1) has equilibrium point $s_1 = (0, 0, 0, 0)$. If $a > 0$, $c > 0$, $d > 0$, $e > 1$, $h > 0$, then it has two other nonzero equilibrium points

$$s_2 = \left(\sqrt{\frac{cde+deh}{e-1}}, \ \sqrt{\frac{cde+deh}{e-1}}, \ \frac{ce+eh}{e-1}, \ -\frac{(c+h)\sqrt{ed(c+h)(e-1)}}{(e-1)^2}\right),$$

$$s_3 = \left(-\sqrt{\frac{cde+deh}{e-1}}, \ -\sqrt{\frac{cde+deh}{e-1}}, \ \frac{ce+eh}{e-1}, \ \frac{(c+h)\sqrt{ed(c+h)(e-1)}}{(e-1)^2}\right).$$

2.2. Symmetry

Note that system (1) is invariant under the coordinate transformation

$$(x, y, z, w) \to (-x, -y, z, -w),$$

i.e., the system is symmetrical about the z axis, so if (x, y, z, w) is a solution of system (1), then $(-x, -y, z, -w)$ is also a solution.

2.3. Dissipation

For the new system (1), it meets the equation

$$\boldsymbol{\nabla} V = \frac{\partial \dot{x}}{\partial x} + \frac{\partial \dot{y}}{\partial y} + \frac{\partial \dot{z}}{\partial z} + \frac{\partial \dot{w}}{\partial w} = -a + h - d + e, \quad (3)$$

that is, the system is dissipative with an exponential contraction rate

$$\frac{\mathrm{d}V}{\mathrm{d}t} = -(a + d - h - e).$$

For any $c \in \mathrm{R}$ and $a + d > h + e$, this means that a volume element V_0 is contracted by the flow into a volume element $V_0\,\mathrm{e}^{-(a+d-h-e)}$ at time t.

3. Pitchfork bifurcation analysis

The Jacobian matrix at s_1 is given by

$$\boldsymbol{J} = \begin{bmatrix} -a & a & 0 & 0 \\ c & h & 0 & -1 \\ 0 & 0 & -d & 0 \\ 0 & 0 & 0 & e \end{bmatrix}, \quad (4)$$

and its characteristic equation is

$$\begin{aligned} &\lambda^4 + (a + d - e - h)\lambda^3 + (ad + eh - ac - ae - ah \\ &\quad - ed - dh + ace + aeh + deh - acd - ade \\ &\quad - adh)\lambda + ade(c + h) = 0. \end{aligned} \quad (5)$$

Obviously, the four roots of Eq. (5) do not always have negative real parts according to the Routh–Hurwitz condition.

3.1. Pitchfork bifurcation at s_1

When $e = 0$, the characteristic equation at $s_1 = (0, 0, 0, 0)$ is simplified to

$$\begin{aligned} f(\lambda) &= \lambda(\lambda^3 + (a + d - h)\lambda^2 \\ &\quad + (ad - ac - ah - dh)\lambda - ad(c + h)) \\ &= 0, \end{aligned} \quad (6)$$

and the eigenvalues of Eq. (6) are

$$\begin{aligned} &\lambda_1 = 0, \quad \lambda_2 = -d, \\ &\lambda_3 = \frac{h - a - \sqrt{a^2 + 2ah + 4ac + h^2}}{2}, \\ &\lambda_4 = \frac{h - a + \sqrt{a^2 + 2ah + 4ac + h^2}}{2}. \end{aligned}$$

The corresponding eigenvectors are

$$\boldsymbol{v}_1 = \begin{bmatrix} \dfrac{1}{c + h} \\ \dfrac{1}{c + h} \\ 0 \\ 1 \end{bmatrix}, \quad \boldsymbol{v}_2 = \begin{bmatrix} 0 \\ 0 \\ 1 \\ 0 \end{bmatrix},$$

$$\boldsymbol{v}_3 = \begin{bmatrix} -\dfrac{a + h + \sqrt{a^2 + 2ah + 4ac + h^2}}{2c} \\ 1 \\ 0 \\ 0 \end{bmatrix},$$

$$\boldsymbol{v}_4 = \begin{bmatrix} -\dfrac{a + h - \sqrt{a^2 + 2ah + 4ac + h^2}}{2c} \\ 1 \\ 0 \\ 0 \end{bmatrix}.$$

Let $\boldsymbol{T} = [\boldsymbol{v}_1 \quad \boldsymbol{v}_2 \quad \boldsymbol{v}_3 \quad \boldsymbol{v}_4]^{\mathrm{T}}$, $[x \quad y \quad z \quad w]^{\mathrm{T}} = \boldsymbol{T}[x_1 \quad x_2 \quad x_3 \quad x_4]^{\mathrm{T}}$, system (1) is transformed into the standard form, we obtain

$$\begin{bmatrix} \dot{x}_1 \\ \dot{x}_2 \\ \dot{x}_3 \\ \dot{x}_4 \end{bmatrix} = \begin{bmatrix} 0 & 0 & 0 & 0 \\ 0 & -d & 0 & 0 \\ 0 & 0 & \dfrac{h - a - \sqrt{a^2 + 2ah + 4ac + h^2}}{2} & 0 \\ 0 & 0 & 0 & \dfrac{h - a + \sqrt{a^2 + 2ah + 4ac + h^2}}{2} \end{bmatrix} \begin{bmatrix} x_1 \\ x_2 \\ x_3 \\ x_4 \end{bmatrix} + \begin{bmatrix} f_1 \\ f_2 \\ f_3 \\ f_4 \end{bmatrix}, \quad (7)$$

and

$$\begin{aligned} f_1 &= ex_1 + \frac{1}{c + h}x_1x_2 - \frac{a + h + \Delta}{2c}x_2x_3 - \frac{a + h - \Delta}{2c}x_2x_4, \\ f_2 &= \frac{1}{(c + h)^2}x_1^2 - \frac{a + h + \Delta}{2c}x_3^2 - \frac{a + h - \Delta}{2c}x_4^2 + \frac{2c - a - h - \Delta}{2c(c + h)}x_1x_3 + \frac{2c - a - h + \Delta}{2c(c + h)}x_1x_4 - \frac{a + h}{c}x_3x_4, \end{aligned}$$

$$
\begin{aligned}
f_3 = {} & \frac{e(a+h+2c-\Delta)}{2(c+h)\Delta}x_1 \\
& + \frac{2c+(c+h+1)(a+h-\Delta)}{2(c+h)^2\Delta}x_1x_2 \\
& + \frac{a-h+2ah+2ac-\Delta}{2(c+h)\Delta}x_2x_3 \\
& - \frac{(a+h-\Delta)^2(c+h+1)+2c(a+h-\Delta)}{4c(c+h)\Delta}x_2x_4, \\
f_4 = {} & \frac{e(a+h+2c+\Delta)}{2(c+h)\Delta}x_1 \\
& - \frac{2c+(c+h+1)(a+h+\Delta)}{2(c+h)^2\Delta}x_1x_2 \\
& + \frac{(a+h+\Delta)^2(c+h+1)+2c(a+h+\Delta)}{4c(c+h)\Delta}x_2x_3 \\
& - \frac{a-h+2ac+2ah+\Delta}{2(c+h)\Delta}x_2x_4,
\end{aligned}
$$

where $\Delta = \sqrt{a^2+2ah+4ac+h^2}$.

In order to investigate pitchfork bifurcation behavior, we reduce the system dimensions by applying the center manifold theorem

$$
\begin{aligned}
W^{\mathrm{c}}(0) = \{&(x_1,x_2,x_3,x_4,e)\in \mathrm{R}^5 | x_2 = h_1(x_1,e), \\
& x_3 = h_2(x_1,e), \quad x_4 = h_3(x_1,e), \\
& |x_1|<\delta, \quad |e|<\bar{\delta}, \quad h_i(0,0)=0, \\
& \mathrm{D}h_i(0,0)=0, \quad i=1,2,3\}, \qquad (8)
\end{aligned}
$$

where δ and $\bar{\delta}$ are sufficiently small. We compute the center manifold and derive the vector field on the center manifold. We assume

$$
\begin{aligned}
x_2 &= h_1(x_1,e) = a_1x_1^2 + a_2x_1e + a_3e^2 + \cdots, \\
x_3 &= h_2(x_1,e) = b_1x_1^2 + b_2x_1e + b_3e^2 + \cdots, \\
x_4 &= h_3(x_1,e) = c_1x_1^2 + c_2x_1e + c_3e^2 + \cdots. \qquad (9)
\end{aligned}
$$

According to the center manifold theorem,[21] the center manifold must satisfy

$$
\boldsymbol{N}(h(x,e)) = \mathrm{D}h[Ax_1+f_1] - \boldsymbol{BH} - \boldsymbol{g} = 0, \qquad (10)
$$

where $A=0$,

$$
\boldsymbol{B} = \begin{bmatrix}
-d & 0 & 0 \\
0 & \dfrac{h-a-\sqrt{a^2+2ah+4ac+h^2}}{2} & 0 \\
0 & 0 & \dfrac{h-a+\sqrt{a^2+2ah+4ac+h^2}}{2}
\end{bmatrix}, \quad
\boldsymbol{H} = \begin{bmatrix} h_1 \\ h_2 \\ h_3 \end{bmatrix}, \quad
\boldsymbol{g} = \begin{bmatrix} f_2 \\ f_3 \\ f_4 \end{bmatrix}.
$$

Substituting Eq. (9) into Eq. (10) and equating the like powers to zero, we obtain

$$
\begin{aligned}
x_1^2: \quad & a_1 = \frac{1}{d(c+h)^2}, \quad b_1 = 0, \quad c_1 = 0; \\
x_1e: \quad & a_2 = 0, \quad b_2 = \frac{a+2c+h-\sqrt{a^2+2ah+4ac+h^2}}{(c+h)\left(a-h+\sqrt{a^2+2ah+4ac+h^2}\right)\sqrt{a^2+2ah+4ac+h^2}}, \\
& c_2 = \frac{a+2c+h+\sqrt{a^2+2ah+4ac+h^2}}{(c+h)\left(a-h-\sqrt{a^2+2ah+4ac+h^2}\right)\sqrt{a^2+2ah+4ac+h^2}}; \\
e^2: \quad & a_3 = 0, \quad b_3 = 0, \quad c_3 = 0.
\end{aligned}
$$

Then we obtain

$$
x_2 = h_1(x_1,e) = a_1x_1^2 + \cdots, \quad x_3 = h_2(x_1,e) = b_2x_1e + \cdots, \quad x_4 = h_3(x_1,e) = c_2x_1e + \cdots. \qquad (11)
$$

Substituting Eq. (11) into the expression of f_1, we obtain the vector field reduced to the center manifold

$$
\begin{aligned}
\dot{x}_1 &= ex_1 - a_1x_1^3\left[\frac{b_2e\left(a+h+\sqrt{a^2+2ah+4ac+h^2}\right)+c_2e\left(a+h-\sqrt{a^2+2ah+4ac+h^2}\right)}{2c} - \frac{1}{h+c}\right] + \cdots, \\
\dot{e} &= 0. \qquad (12)
\end{aligned}
$$

According to the bifurcation theory, we can easily verify that the following conditions are satisfied for the equilibrium point $(x_1,e)=(0,0)$ of Eq. (12) to undergo a pitchfork bifurcation at $e=0$. Let $(x_1,e)=(0,0)$,

then at $s_1 = (0, 0, 0, 0)$, we have

$$F(0,0) = 0,\ \left.\frac{\partial F}{\partial x_1}\right|_{(0,0)} = 0,\ \left.\frac{\partial F}{\partial e}\right|_{(0,0)} = 0,\ \left.\frac{\partial^2 F}{\partial x_1^2}\right|_{(0,0)} = 0,\ \left.\frac{\partial^2 F}{\partial x_1 \partial e}\right|_{(0,0)} = 1 \neq 0,\ \left.\frac{\partial^3 F}{\partial x_1^3}\right|_{(0,0)} = \frac{6}{d(c+h)^3} \neq 0,$$

where

$$F(x_1, e) = ex_1 - a_1 x_1^3 \left[\frac{b_2 e(a+h+\sqrt{a^2+2ah+4ac+h^2}) + c_2 e(a+h-\sqrt{a^2+2ah+4ac+h^2})}{2c} - \frac{1}{h+c}\right].$$

Thus, the conditions of the pitchfork bifurcation are satisfied, system (1) undergoes a pitchfork bifurcation at $s_1 = (0, 0, 0, 0)$. Therefore, we obtain the following theorem.

Theorem 1 For $e = 0$, system (1) undergoes a pitchfork bifurcation at $s_1 = (0, 0, 0, 0)$. Moreover, for $e < 0$, there is only one stable equilibrium point $s_1 = (0, 0, 0, 0)$, for $e > 0$, there are three equilibrium points $s_1 = (0, 0, 0, 0)$,

$$s_2 = \left(\sqrt{\frac{cde+deh}{e-1}}, \sqrt{\frac{cde+deh}{e-1}}, \frac{ce+eh}{e-1}, -\frac{(c+h)\sqrt{ed(c+h)(e-1)}}{(e-1)^2}\right),$$

$$s_3 = \left(-\sqrt{\frac{cde+deh}{e-1}}, -\sqrt{\frac{cde+deh}{e-1}}, \frac{ce+eh}{e-1}, \frac{(c+h)\sqrt{ed(c+h)(e-1)}}{(e-1)^2}\right),$$

where s_1 is unstable, and both s_2 and s_3 are stable near $e = 0$.

3.2. Numerical simulation

In order to observe pitchfork bifurcation behavior, we set $a = 35$, $c = -15$, $d = 6$, $h = 12$, and vary parameter e in $[-1,\ 0.6]$. As shown in Fig. 2, we obtain the pitchfork bifurcation behavior. According to Theorem 1, system (1) has only one stable equilibrium point s_1 when $e < 0$; and when $e > 0$, system (1) has three equilibrium points s_1, s_2, and s_3, s_1 is unstable, s_2, s_3 are stable.

To verify the theoretical analysis, we set $a = 35$, $c = -15$, $d = 6$, $h = 12$, $e = -0.5$, and choose $i_1 = (1, 1, 1, 1)$ and $i_2 = (-1, -1, -1, -1)$ as two different initial points, which are not in the neighborhood of the zero equilibrium point. As shown in Fig. 3(a), we find that the system trajectories converge to the stable equilibrium point s_1.

Let $a = 35$, $c = -15$, $d = 6$, $h = 12$, and $e = 0.5$, the equilibrium points s_2, s_3 should be stable. We choose $i_2 = (-1, -1, -1, -1)$ as the initial point, Figure 3(b) shows that the system orbit runs away from equilibrium point s_1 and is attracted to equilibrium point s_2. When we choose $i_1 = (1, 1, 1, 1)$ as the initial point, the system orbit is attracted to equilibrium point s_3 as shown in Fig. 3(c). Thus, all the results of the numerical simulations are in accord with Theorem 1, that is to say, system (1) doe indeed undergo a pitchfork bifurcation.

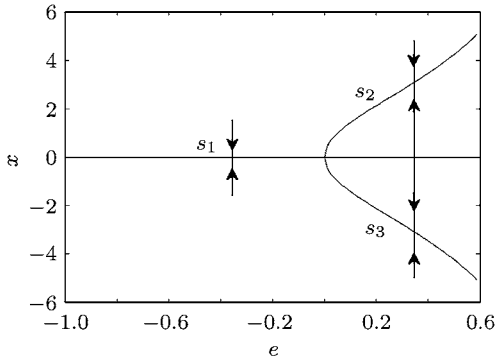


Fig. 2. Pitchfork bifurcation diagram near $e = 0$, with $a = 35$, $c = -15$, $d = 6$, $h = 12$.

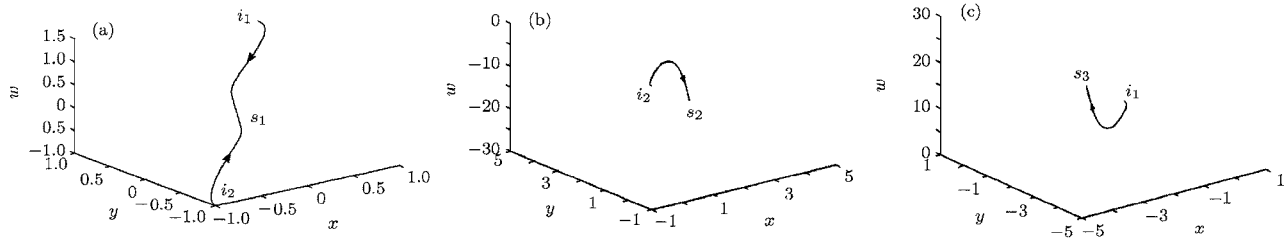


Fig. 3. Dynamical behaviors of system (1) with $a = 35$, $c = -15$, $d = 6$, $h = 12$, (a) $e = -0.5$, initial points $i_1 = (1, 1, 1, 1)$ and $i_2 = (-1, -1, -1, -1)$, (b) $e = 0.5$, initial point $i_2 = (-1, -1, -1, -1)$, and (c) $e = 0.5$, initial point $i_1 = (1, 1, 1, 1)$.

4. Numerical bifurcation analysis

For a hyper-chaotic system, its dynamical properties can be illustrated by the Lyapunov exponent spectrum and the numerical bifurcation diagram. In this section, we choose parameters c and e as the adjustable parameters.

4.1. Analysis with respect to c

In this section, $a = 35$, $d = 6$, $e = 2$, $h = 12$, and c is varied, we find that the system can generate hyper-chaotic dynamical behaviors in a wide region of c. As shown in Fig. 4, system (1) can evolve into chaotic and hyper-chaotic behaviors alternately. When $c \in [0, 2.4] \cup (11, 26]$, only the largest Lyapunov exponent is positive, which implies that the system is chaotic; when $c \in (2.4, 11] \cup (26, 100]$, system (1) has two positive Lyapunov exponents, which indicates that the system is hyper-chaotic. Figure 5 shows the different attractors of system (1) with different c.

4.2. Analysis with respect to e

Let $a = 35$, $c = 7$, $d = 6$, $h = 12$, and vary e, we find that system (1) can generate complex dynamical behaviors. Especially, the phenomenon of direct transition from quasi-periodic behaviors to hyper-chaotic behaviors is found. As shown in Fig. 6, system (1) can evolve into quasi-periodic and hyper-chaotic attractors. When $e \in [-2, 0.5]$, the two largest Lyapunov exponents of system (1) are approximately equal to zero, which indicates that the system is quasi-periodic.

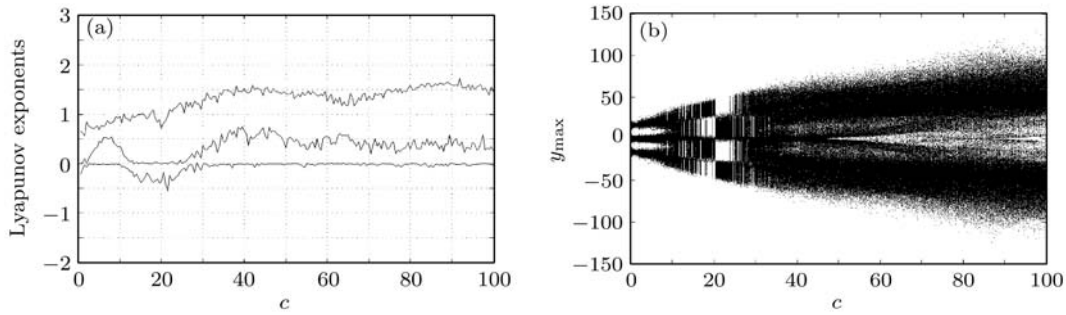


Fig. 4. (a) Lyapunov exponent spectrum and (b) bifurcation diagram obtained when $a = 35$, $d = 6$, $e = 2$, $h = 12$, and $0 \le c \le 100$.

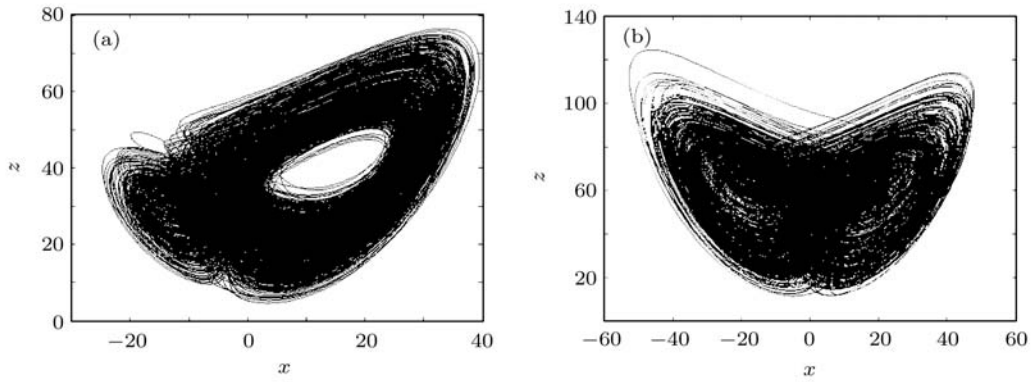


Fig. 5. (a) Chaotic attractor with $c = 20$ in x–z plane, and (b) hyper-chaotic attractor with $c = 40$ in x–z plane, where $a = 35$, $d = 6$, $e = 2$, $h = 12$.

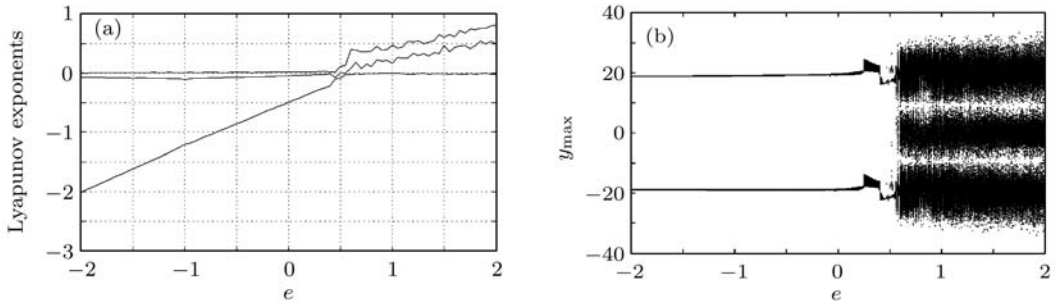


Fig. 6. (a) Lyapunov exponent spectrum and (b) bifurcation diagram when $a = 35$, $c = 7$, $d = 6$, $h = 12$, $-2 \le e \le 2$.

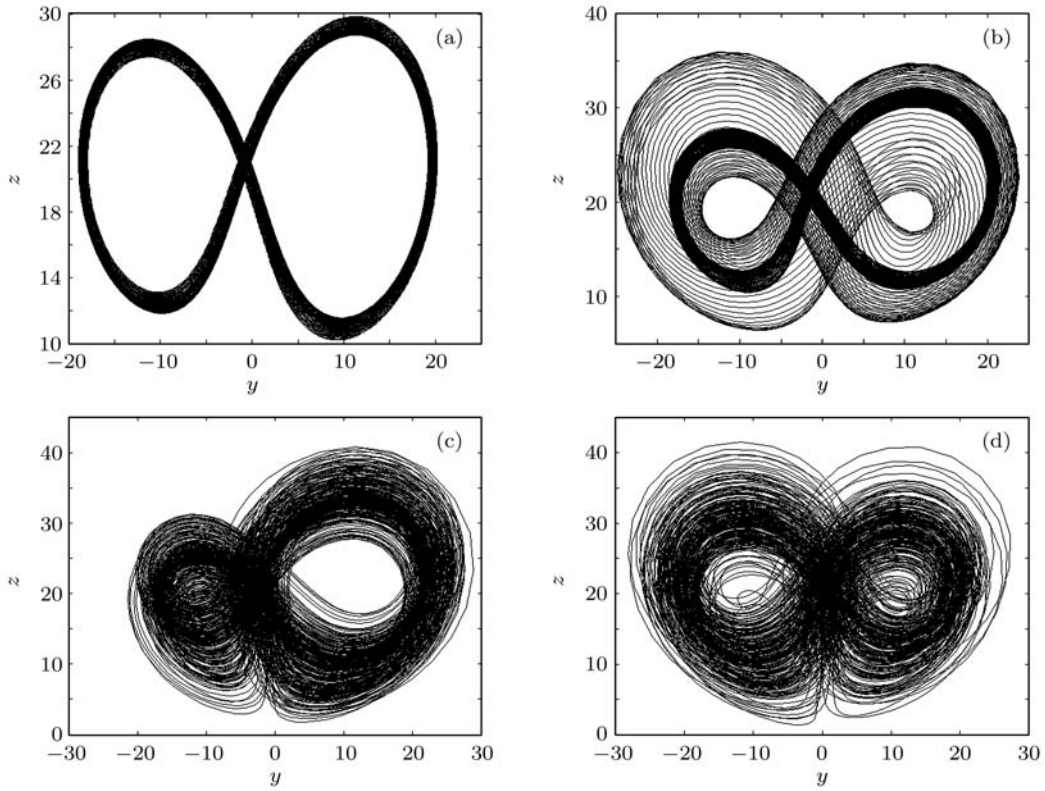


Fig. 7. Various attractors in system (1) with $a = 35$, $c = 7$, $d = 6$, $h = 12$, (a) $e = -0.5$, quasi-periodic attractor in y–z plane; (b) $e = 0.5$, quasi-periodic attractor in y–z plane; (c) $e = 1.0$, hyper-chaotic attractor in y–z plane; and (d) $e = 1.5$ hyper-chaotic attractor in y–z plane.

When $e \in (0.5, 2]$, system (1) has two positive Lyapunov exponents, and the system is hyper-chaotic. System (1) has an interesting dynamical evolution process when e increases, Figure 7 shows some typical attractors of system (1).

5. Circuit implementation

For the convenience of engineering applications, an electric circuit is designed in this section. As shown in Fig. 8, the circuit consists of four channels to implement the integration, addition, and subtraction of the state variables x, y, z, and w respectively. Obviously, state variables x, y, z, and w in system (1) correspond to the state voltages of the four channels, respectively. Considering the saturation property of the analog multipliers and the operational amplifier, we reduce the state variables of system (1) tenfold by using a linear transformation. The original system (1) is transformed into

$$\begin{aligned} 0.1\dot{\tilde{x}} &= 3.5(\tilde{y} - \tilde{x}), \\ 0.1\dot{\tilde{y}} &= 0.7\tilde{x} + 1.2\tilde{y} - \tilde{x}\tilde{z} - 0.1\tilde{w}, \\ 0.1\dot{\tilde{z}} &= \tilde{x}\tilde{y} - 0.6\tilde{z}, \\ 0.1\dot{\tilde{w}} &= \tilde{x}\tilde{z} + 0.2\tilde{w}. \end{aligned} \tag{13}$$

According to Eq. (13), the equations of the circuit can be described as

$$\begin{aligned} R_3C_1\dot{\tilde{x}} &= \frac{R_5}{R_1}\tilde{y} - \frac{R_1 + R_5}{R_1}\frac{R_{25}}{R_{20} + R_{25}}\tilde{x}, \\ R_7C_2\dot{\tilde{y}} &= \frac{R_9R_{26} + R_{10}R_{26}}{R_2R_{10}}\frac{R_6R_8R_{29}}{R_6R_8 + R_6R_{29} + R_8R_{29}} \\ &\quad \times \left(\frac{\tilde{x}}{R_8} + \frac{\tilde{y}}{R_6}\right) - \frac{R_9R_{26}}{R_2R_{10}}\tilde{x}\tilde{z} \\ &\quad - \frac{R_2 + R_{26}}{R_2}\frac{R_{11}}{R_{11} + R_{28}}\tilde{w}, \\ R_{13}C_3\dot{\tilde{z}} &= \frac{R_{15}}{R_{12}}\tilde{x}\tilde{y} - \frac{R_{12} + R_{15}}{R_{12}}\frac{R_{14}}{R_{14} + R_{17}}\tilde{z}, \\ R_{22}C_4\dot{\tilde{w}} &= \frac{R_{24}}{R_{21}}\tilde{x}\tilde{z} - \frac{R_{24}}{R_{23}}\tilde{w}, \end{aligned} \tag{14}$$

where the values of resistors and capacitors are R_1, R_2, R_9, R_{11}, R_{14}, R_{15}, R_{20}, R_{24}, R_{26}, $R_{29} = 1\ \mathrm{k}\Omega$, R_3, R_7, R_{13}, $R_{22} = 100\ \mathrm{k}\Omega$, R_5, $R_{25} = 3.5\ \mathrm{k}\Omega$, R_{10}, R_{12}, $R_{21} = 100\ \Omega$, $R_6 = 7.58\ \mathrm{k}\Omega$, $R_8 = 13\ \mathrm{k}\Omega$, $R_{17} = 17.33\ \mathrm{k}\Omega$, $R_{23} = 5\ \mathrm{k}\Omega$, $R_{28} = 19\ \mathrm{k}\Omega$, and C_1, C_2, C_3, $C_4 = 470$ pF.

As shown in Fig. 9, the hyper-chaotic attractors observed by an oscilloscope show great consistence with the attractors in Fig. 1, which demonstrates the existence of the Chen hyper-chaotic system.

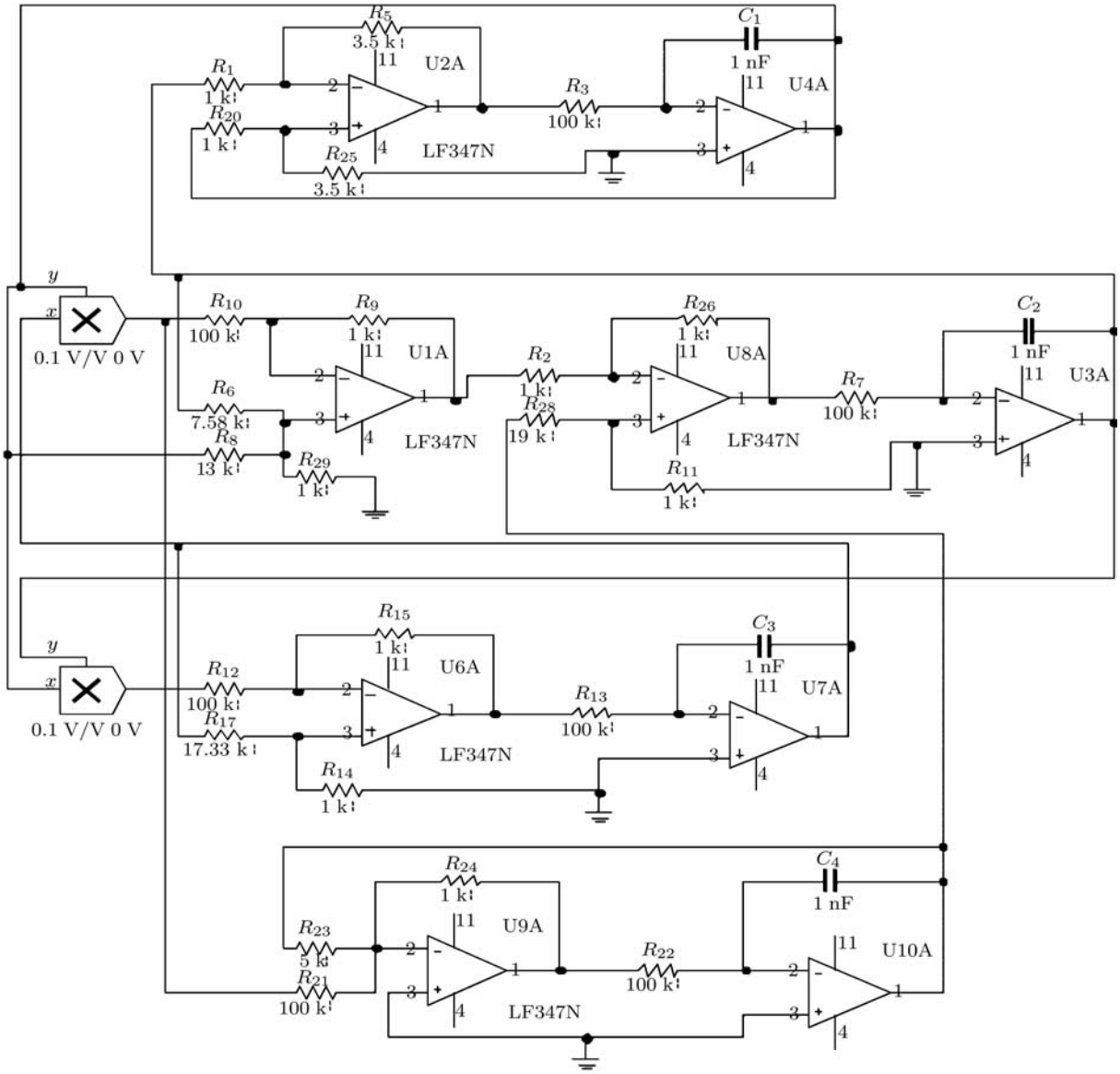


Fig. 8. Circuit diagram of the Chen hyper-chaotic system.

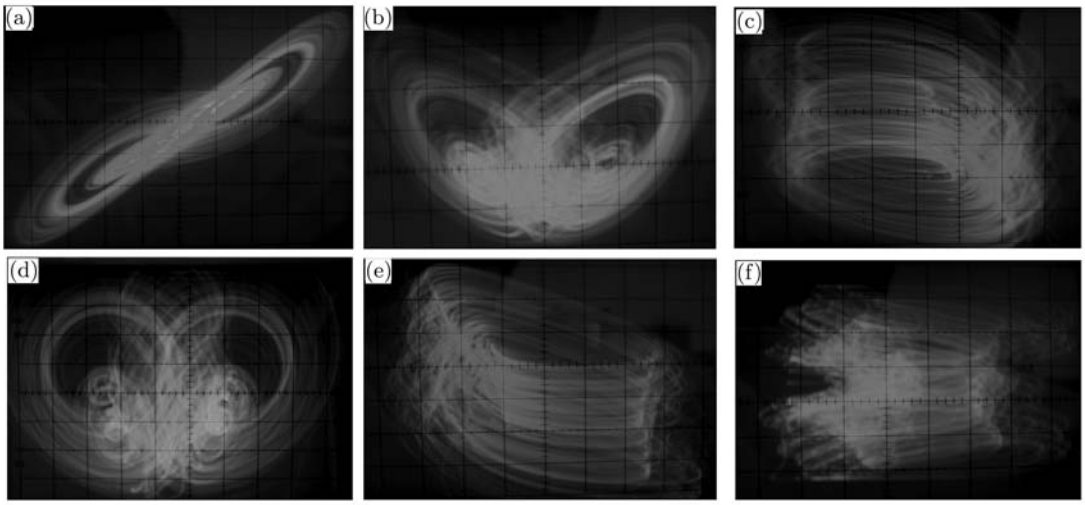


Fig. 9. Chen hyper-chaotic attractors in (a) x–y, (b) x–z, (c) x–w, (d) y–z, (e) y–w, and (f) z–w planes measured by an oscilloscope.

6. Conclusion

In this paper, a new Chen hyper-chaotic system is generated by introducing a state variable w into the Chen system. First, some basic properties of the new system have been discussed, such as symmetry, equilibrium, and dissipation. The pitchfork bifurcation behavior of this new system has been investigated by using the center manifold theorem and the local bifurcation theory. The theoretical analysis demonstrates that the new system can undergo a pitchfork bifurcation at $s_1 = (0, 0, 0, 0)$. The numerical bifurcations have been analyzed when parameter c or e is varied, and the simulation results show that the system has complex dynamical behaviors, such as a wide hyper-chaotic parameter region, a direct transition from quasi-periodic behavior to hyper-chaotic behavior. Finally, an electric circuit is designed to physically implement the new hyper-chaotic system, the experimental results show great consistence with the numerical simulations. Due to the complex dynamic behaviors, this system has broad application prospects in the field of secure communication.

References

[1] Lorenz E N *Atmos. Sci.* **20** 130

[2] Chua L, Komuro M and Matsumoto T 1986 *IEEE Trans. Circuit Sys.* I **33** 1072

[3] Ott E, Grebogi C and Yorke J A 1990 *Phys. Rev. Lett.* **64** 1196

[4] Li Y X, Liu X Z and Zhang H T 2005 *Math. Comput. Mod.* **42** 1359

[5] Song Y Z 2010 *Chin. Phys.* B **19** 060513

[6] Zhang Q L, Lv L and Zhang Y 2011 *Chin. Phys.* B **20** 090514

[7] Zhang J X and Tang W S 2009 *Chaos Soliton. Fract.* **42** 2181

[8] Qi G Y, Chen G R, van Wyk M A, van Wyk B J and Zhang Y H 2008 *Chaos Soliton. Fract.* **38** 705

[9] Wang X Y and Gao Y F 2010 *Commun. Nonlinear Sci. Numer. Simulat.* **15** 99

[10] Chen G R and Mao Y B 2004 *Chaos Soliton. Fract.* **21** 749

[11] Funakoshi M 2008 *Fluid Dyn. Res.* **40** 1

[12] Zhao Z, Yang L and Chen L S 2011 *Nonlinear Dyn.* **63** 521

[13] Yang X S, Li Q D and Chen G R. 2003 *Int. J. Circuit Theory Application* **31** 637

[14] Li Y X, Tang W K S and Chen G R 2005 *Int. J. Bifurcat Chaos* **15** 3367

[15] Chen Z Q, Yang Y, Qi G Y and Yuan Z Z 2007 *Phys. Lett.* A **360** 696

[16] Wu W J and Chen Z Q 2010 *Nonlinear Dyn.* **60** 615

[17] Yu S M, Lin Q H and Qiu S S 2003 *Acta Phys. Sin.* **52** 25 (in Chinese)

[18] Liu C X and Liu L 2009 *Chin. Phys.* B **18** 2188

[19] Qi G Y, van Wyk M A, van Wyk B J and Chen G R 2009 *Chaos Soliton. Fract.* **40** 2544

[20] Chen G R and Ueta T 1999 *Int. J. Bifurcat Chaos* **9** 1465

[21] Wiggins S 1990 *Introduction to Applied Nonlinear Dynamical Systems and Chaos* (New York: Springer-Verlag) pp. 253–270